Analytical Correction of Banding Artifacts in Driven Equilibrium Single Pulse Observation of T2 (DESPOT2)

Jean-David Jutras[1], Keith Wachowicz[1,2], and Nicola DeZanche[1,2]

[1]*Oncology, University of Alberta, Edmonton, AB, Canada,* [2]*Medical Physics, Cross Cancer Institute, Edmonton, AB, Canada*

Purpose: The DESPOT2 (single-component) technique consists of varying the flip angle in bSSFP and solving for T_2 using the on-resonance bSSFP signal equation and previously-measured T_1 (e.g., DESPOT1) [1]. However, banding artifacts induced by B_0 inhomogeneity, especially at 3T and higher fields [2], result in bands of underestimated T_2. A previous approach to correct this problem consists of acquiring 2 phase-cycled bSSFP images at 2 different flip angles and curve-fitting T_2 and off-resonance phase ϕ using a stochastic region contraction algorithm [2]. Here, we perform the same correction analytically and therefore more efficiently.

Theory: Because of off-resonance (Δf), the T_2 normally calculated from the linearized on-resonance bSSFP equation [1] becomes a reduced T_2 or "τ_2" given by Eq. (2) below, where $E_2=\exp(-TR/T_2)$. Solving for τ_2 using bSSFP images at two or more flip angles and phase cycles (e.g., α_1/α_2 at phase cycle increment of $\Delta\phi_1$, and α_1/α_2 at $\Delta\phi_2$) separated by a phase-increment difference $\Delta\phi_2-\Delta\phi_1=\pi$, an exact solution for T_2 and ϕ can be written

$$T_2 = -TR/\ln\left(\sqrt{\frac{2\varepsilon_2^{\Delta\phi_1}\varepsilon_2^{\Delta\phi_2}-\varepsilon_2^{\Delta\phi_1}-\varepsilon_2^{\Delta\phi_2}}{\varepsilon_2^{\Delta\phi_1}+\varepsilon_2^{\Delta\phi_2}-2}}\right),\quad \cos(\phi-\Delta\phi_1)=\frac{\varepsilon_2^{\Delta\phi_1}-\varepsilon_2^{\Delta\phi_2}}{\sqrt{(\varepsilon_2^{\Delta\phi_1}+\varepsilon_2^{\Delta\phi_2}-2)(2\varepsilon_2^{\Delta\phi_1}\varepsilon_2^{\Delta\phi_2}-\varepsilon_2^{\Delta\phi_1}-\varepsilon_2^{\Delta\phi_2})}} \qquad (1a,b)$$

where $\varepsilon_2^{\Delta\phi}=\exp(-TR/\tau_2^{\Delta\phi})$, and $\phi=2\pi\,TR\,\Delta f$. Alternatively, an approximate weighted root-sum-of-squares (wRSS) solution for T_2 can also be derived for 3 or more phase cycles, assuming $TR \ll T_2$, and only deviates by <1% in vivo (Eq. 3):

$$\tau_2(\phi,TR,T_2) = -TR/\ln\left(\frac{E_2+\cos\phi}{E_2^{-1}+\cos\phi}\right), \qquad (2) \qquad T_2 \cong \sqrt{\frac{8}{3N}}\sqrt{\sum_{n=1}^{N}\left(\tau_2^{\Delta\phi_n}\right)^2}, \quad N\geq 3 \qquad (3)$$

where N is the number of phase cycles used. Equation 3 yields more uniform T_2-to-noise ratio (T2NR) than Eq. 1 (**Figure 1**).

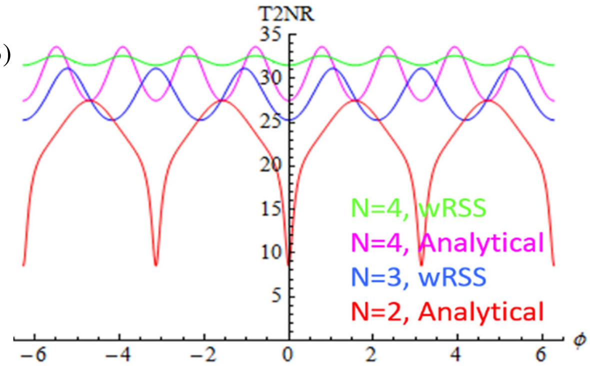

Figure 1: Predicted T2NR as a function of ϕ, for different numbers of phase cycles, ($T_1/\sigma_1/T_2$=1000/10/70ms) and a bSSFP noise factor σ/M_0=0.002.

Methods: The generalized DESPOT2 method was tested (without shimming) on a Philips 3T Achieva, on an agar phantom and on the brain of a healthy volunteer for two ($\Delta\phi$=0, π), three ($\Delta\phi$=0, $2\pi/3$, $4\pi/3$) and four ($\Delta\phi$=0, $\pi/2$, π, $3\pi/2$) phase cycles and (α_1/α_2=13/65°, TR/TE=4.6/2.3 ms, BW=675 Hz/pix), thus totalling 6×2=12 datasets (<2 min each); T_1 was mapped using a 9-echo SPGR pulse sequence: TR/ΔTE=33/2.3 ms, α_1/α_2=5/28°, BW=517 Hz/pix, FOV=24×24×17 cm^3 and voxel resolution: 1×1×1.5 mm^3. Transmit B_1-inhomogeneity was corrected using Actual Flip Angle Imaging [3]. A gold-standard T_2 map was also measured in the phantom using a 10-echo CPMG pulse sequence (TR/ΔTE = 2000/20 ms). Monte Carlo noise simulations were performed in MATLAB to verify the analytical prediction of T2NR as a function of ϕ.

Results and Discussion: The analytical predictions on T2NR (shown in Figure 1) agreed well with the simulations. While further work is underway to address the residual ripples (as seen in **Figure 2c** & **d**, and green ellipse in **3**), the generalized DESPOT2 technique agrees to within 7% of CPMG values within the range of $20\leq T_2\leq 200$ ms.

Conclusion: These analytical solutions yield 3D T_2 and ϕ maps in ~20 s and overcome the limitations of traditional DESPOT2. Applications include 3D structural brain and musculosceletal imaging where motion is not an issue.

References: [1] S. Deoni, B. Rutt, T. Peters. MRM 2003; 49(3):515-526. [2] S. Deoni. JMRI 2009; 30(2):411-417. [3] V. Yarnykh. MRM 2007; 57(1):192-200.

Acknowledgements: the Alberta Cancer Foundation for funding; GyroTools and Philips Healthcare for technical support.

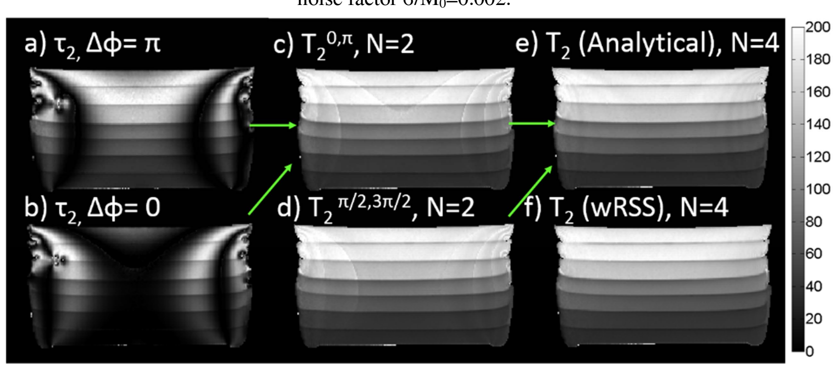

Figure 2: τ_2 maps (left) and T_2 maps in phantom (middle & right). Note that (e) is an optimally weighted average of (c) and (d), while (f) is the approximate wRSS solution.

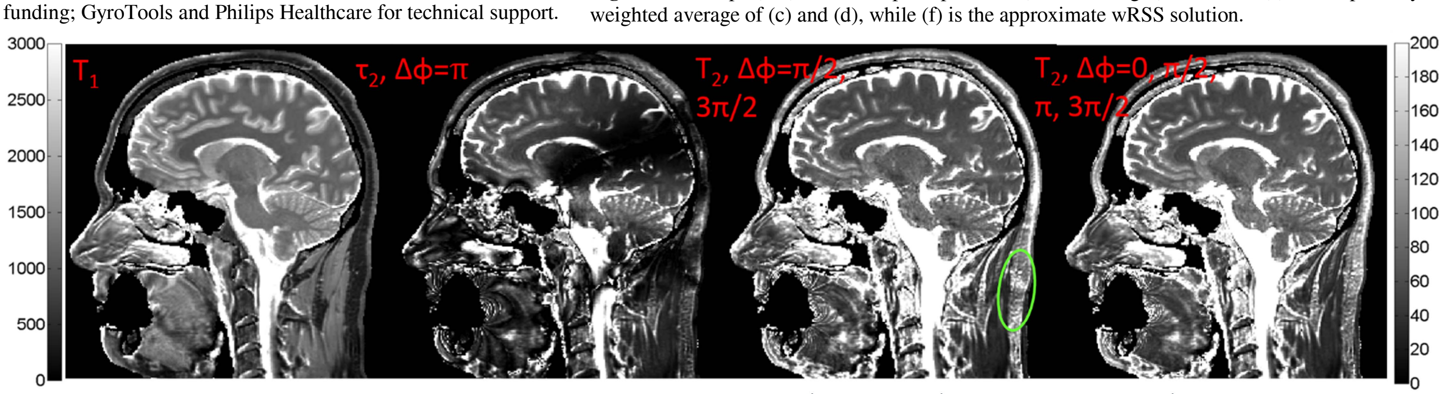

Figure 3: Relaxation times (in ms) in the brain of a volunteer (from left to-right: T_1, τ_2 with $\Delta\phi=\pi$, T_2 with $\Delta\phi=\pi/2$, $3\pi/2$, and T_2 with $\Delta\phi$=0, $\pi/2$, π, $3\pi/2$ (wRSS).